Available online at http://www.biij.org/2012/3/e20
doi: 10.2349/biij.8.3.e20

biij
Biomedical Imaging and Intervention Journal
REVIEW ARTICLE

Challenges in the delivery of radical radiotherapy for locally advanced non-small cell lung cancer

Tho LM*[, 1, 2, 4], McJury M[1], Ho GF[4], Han S[3], Muirhead R[1]

1 Beatson West of Scotland Cancer Centre, United Kingdom
2 Institute of Cancer Sciences, University of Glasgow, United Kingdom
3 West of Scotland PET-CT Centre, United Kingdom
4 University of Malaya Cancer Research Institute, Malaysia

Received 14 March 2012; accepted 15 June 2012

ABSTRACT

Locally advanced non-small cell lung cancer (NSCLC) encompasses a heterogeneous collection of tumour and nodal stages. Despite recent advances, the overall survival for this group remains poor. Radical radiotherapy remains the mainstay of treatment. The complexities involved in the delivery of radical radiotherapy to the lung pertain to tumour volume definition, intra- and inter-fraction motion (namely tumour motion caused by respiration and GTV migration during treatment) and the proximity of organs at risk to the high-dose region. Here we discuss a selection of strategies to manage these complexities. Motion management can be addressed by 4D CT planning, radiotherapy gating and on-board imaging, including cone beam CT. Advanced planning methods such as intensity modulated radiotherapy may potentially allow dose escalation and sparing of normal tissue toxicity. Functional imaging has already improved our ability to stage tumours and more carefully select appropriate candidates for radical treatment. Better imaging also improves GTV definition. However, the complexities of image acquisition and interpretation need to be accounted for and agreed consensus protocols have yet to be defined. Novel imaging methods such as 4D PET-CT and 4D MRI may also yield improvements for the future and these are briefly discussed.

Keywords: Lung cancer; 4DCT; IMRT; respiratory gating; PET-CT.

INTRODUCTION

Locally advanced non-small cell lung cancer (NSCLC) encompasses a heterogeneous group of patients. In the recently introduced seventh edition of the UICC/AJCC TNM classification, Stage III NSCLC tumours can include large primary tumours with no nodal infiltration to smaller tumours with extensive unilateral, mediastinal or contralateral nodal involvement [1, 2]. For the purposes of this article, locally advanced NSCLC includes patients with unresectable disease, unsuitable for stereotactic body radiotherapy due to size or presence of nodal disease but where all areas of tumour can still be encompassed within a radical radiotherapy field.

The therapeutic approach used in managing these patients can vary widely, nevertheless radical radiotherapy remains the mainstay of curative treatment [3]. There have been numerous advances over recent years, including the significant technical advances in

* Corresponding author. Address: Beatson West of Scotland Cancer Centre, 1053 Great Western Road, Glasgow, G12 0YN, United Kingdom. E-mail: lyetho@gmail.com (Lye Mun Tho).

radiation planning and delivery [4], the use of advanced imaging to better stage and localise tumours for treatment and the introduction of multimodality treatment . Despite this, the 3-year overall survival in Stage III NSCLC remains poor at 31% [5]. We will discuss a small selection of strategies to manage the complexities involved in delivering radical radiotherapy to the lung.

COMPLEXITIES OF LUNG IRRADIATION

The complexities of lung irradiation are due to a number of factors:

1) Target delineation performed by clinicians at planning can have significant inter-clinician variation. In the lung, identifying gross tumour is challenging especially when there has been lung collapse or atelectasis [6]. Steenbakkers *et al*. [7] demonstrated a disagreement of 45% between 11 radiation oncologists, routinely treating lung cancer, who had been given identical clinical and diagnostic information prior to delineating 22 lung tumours. Vorwerk *et al*. [8] confirmed the significant inter-clinician variation and found that although repeated discussions of patient cases and uniform teaching improved the variation, a significant difference remained.
2) Respiration-induced tumour motion complicates lung irradiation. Previous studies have demonstrated that the motion of lung tumours cannot be predicted by tumour size, location or pulmonary function and additional imaging would be required to quantify this accurately [9, 10]. Liu *et al*. [11] assessed the motion of 166 lung tumours and found that 39.2% moved more than 0.5cm in the superior-inferior (SI) direction and 10.8% moved more than 1cm in the SI direction. Lymph node motion must also be considered. Pantarotto *et al*. [12] demonstrated average 3-dimensional nodal motion to be 0.68cm (0.17 – 1.64cm). Bosmans *et al*. [13] demonstrated a similar result with average nodal motion reported as 0.56cm. There are various methods that have been used over the years to image motion such as fluoroscopy [14] or the use of six standard helical computed tomography (CT) scans in combination [15]; however, over the last decade, 4-dimensional (4D) CT planning has increasingly been used to individualise the margin for tumour motion [16, 17]. However a 4D CT only provides a representation of motion over a limited period of time and respiratory variation can occur throughout planning and treatment. Therefore, there has to be an awareness of this potential source of error, with strategies to identify and manage it [18, 19].
3) The final major limiting factor is dose to organs at risk (OARs). Pooled toxicity data has been used to derive maximum tolerated dose to the lung. By convention, the volume of normal lung receiving 20Gy (V20) should not exceed 35% to 37% and the mean lung dose (MLD) should be below 20 to 23Gy [4]. There is no consensus on the maximum tolerated dose to the oesophagus and heart [4]. In routine clinical practice, doses are usually fixed/protocolised ie. provided OAR doses are within tolerance, the standard dose is delivered. Due to uncertainty arising from inter-clinican variation and tumour motion, generous planning target volume (PTV) margins are often required. The need for larger PTV volumes often makes it harder to achieve OAR tolerances and thus may preclude borderline patients from receiving radical treatment. Moreover as radical doses tend to be "inclusive" (to accommodate the majority of patients) this is often limited by the minority of patients with large PTVs with OAR at greater risk. Similar constraints do not apply where OAR tolerances can be easily achieved, and in these cases clinicians have wondered about the potential benefit of dose escalation. This has prompted a number of dose escalation trials where individualised doses are delivered, depending on individualised OAR tolerances [20–23].

The challenge of radiotherapy in locally advanced NSCLC is to manage the complexities of lung irradiation, as described above. New imaging techniques to visualise and manage motion and reduce inter-clinican variation; as well as novel planning and delivery techniques which reduce dose to OAR can all be used with the intention of facilitating dose escalation which improves our local control and, as a result, overall survival [23].

4D CT PLANNING AND ON BOARD IMAGING

During treatment there are a number of potential errors that can result from tumour motion that require different imaging techniques to identify and manage. Firstly there is a potential variation in intra-fraction tumour motion. This is primarily respiration-induced tumour motion, and to some extent, hysteresis and heart motion.

Four-dimensional CT (4D CT) [16] planning is one strategy to deal with intra-fraction motion. The patient undergoes respiratory monitored CT scanning in the treatment position to acquire temporal and spatial information relating to tumour excursion during the breathing cycle (Figure 1). 4D CT image acquisition protocols have been described extensively in the literature, including the methodology employed in our centre [17, 24]. In terms of target volume definition, gross internal target volume (GiTV or iGTV) [16, 25] has been proposed as a novel concept when 4D CT planning is employed (Figure 2). GTV is volumed but expanded to account for positional variation during respiration (expanding the original volume on each respiratory phase or voluming on maximum intensity projection) to account for a composite gross and internal tumour volume [17]. This is then expanded using conventional margins to account for microscopic spread (clinical target volume or CTV) and set-up error to generate PTV. Although a 4D CT performed at planning is useful to visualise motion, it remains a snap-shot in

time and may not necessarily reflect motion during treatment.

Several studies have documented systematic intra-fraction tumour motion error. Michalski *et al*. [18] reported a tumour motion reproducibility of 87%. Bosmans *et al*. [26] reported that although a small number of changes in tumour motion were seen over the course of treatment, in only 4% of patients this would have resulted in an increase of the internal margin. Guckenberger *et al*. [19] found that the mean peak-to-peak tumour motion changed by only 0.9mm on two different scans. Sonke *et al*. [27] reported that the mean variability of the tumour trajectory shape did not exceed 1mm (1 SD). All these papers suggest that in the vast

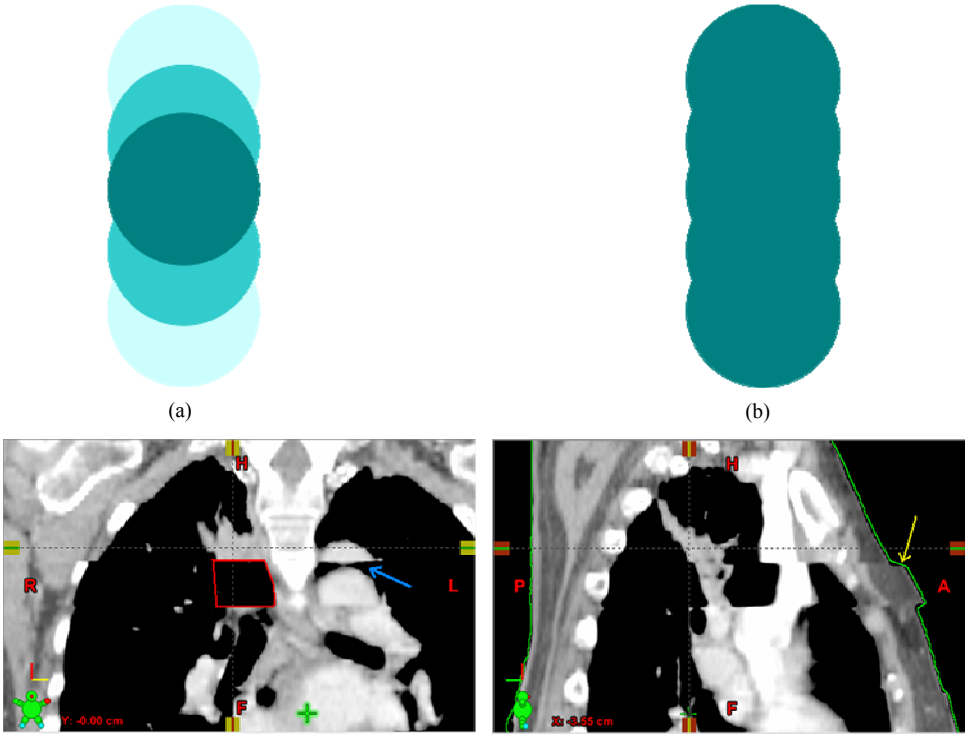

Figure 1 4 Dimensional Computed Tomography (4D CT) and Artefacts Caused by Mismatch of Phase Information. a) 4DCT Average Intensity Projection (Ave-IP) : average pixel value over all phases representing the time-weighted location of the tumour. b) 4D CT Maximum Intensity Projection (MIP) : maximum pixel value over all phases representing all areas traversed by tumour. c) Coronal (left) and sagittal (right) image example from a patient, showing where the tumour mass is incomplete in the image (red box). Another tissue mass (blue arrow) shows an incomplete mass and/or duplication occurring in the same axial image slice. The yellow arrow shows on the sagittal image where the misplacement of the image slice has occurred. These artefacts demonstrate a mismatch of phase information between slices.

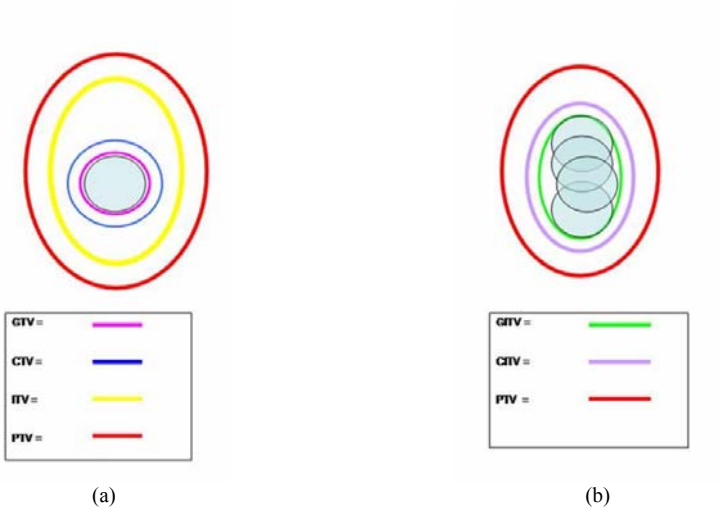

Figure 2 Gross Internal Tumour Volume (GiTV aka iGTV). a) Conventionally GTV is volumed on a single, fast CT scan acquired at planning. It is grown to account for microscopic spread (CTV), respiratory movement (ITV) and set-up errors to achieve a PTV. b) The concept of GiTV or iGTV has been proposed in relation to target volume definition when 4D CT is used for planning. Here GTV is volumed and expanded for each phase of respiration, taking into account tumour excursion during the breathing cycle. This produces the GiTV or iGTV. This is then grown using conventional margins to account for microscopic spread (CTV) and set-up errors (PTV).

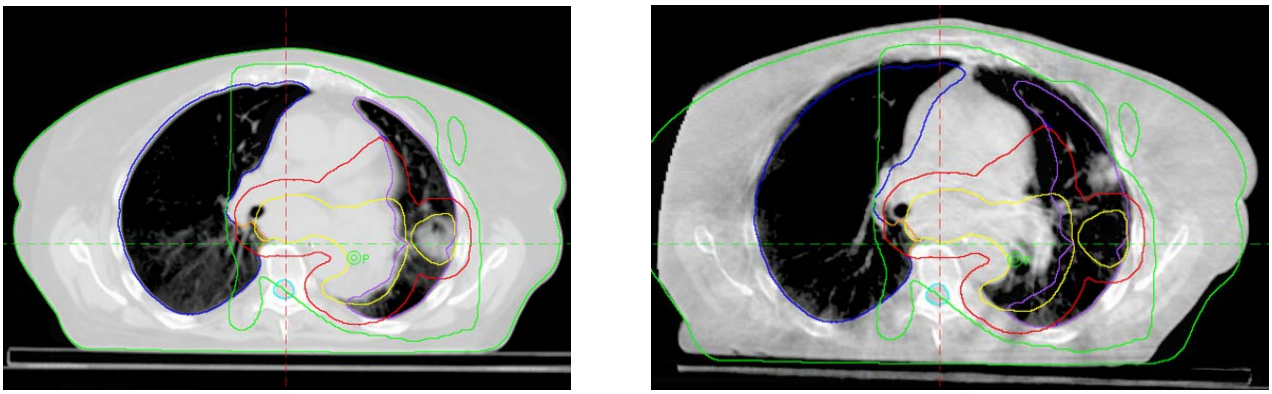

(a) (b)

Figure 3 Inter-Fraction Tumour Migration Detected using On Board (kV) Cone Beam CT Imaging. a) Cone beam CT on first fraction of radiotherapy for non-small cell lung carcinoma demonstrating satisfactory coverage of target. b) A further cone beam CT at fraction 6 now clearly demonstrates that the primary tumour has now migrated out of the PTV.

majority of patients, it is safe to perform a single 4D CT planning scan and complete treatment without re-imaging the intra-fraction motion. However, to identify the few patients with significant errors, imaging can either be performed prior to or during the first few fractions of treatment. This can be performed by cone beam CT, 4D cone beam CT, MV cine-images, fluoroscopy or a repeat 4D CT [18, 26, 28–31].

Inter-fraction tumour motion is a further potential error. Tumour migration and volume change during the course of 4–7 weeks of radiation is a recognised phenomenon. This migration can be an increase or decrease in tumour volume or a migration of the central axis as a result of various factors for example weight loss, inflammation or lung re-expansion. Figure 3 demonstrates a cone beam CT on first fraction and further cone beam CT at fraction 6 where the primary tumour has migrated out of the PTV. Sonke *et al.* [27] reported that the mean inter-fraction tumour migration of the volumes was 1.6mm (left-right), 3.9mm (cranio-caudal) and 2.8mm (anterior/posterior). Britton *et al.* [32] found results that were not too dissimilar, with migration of the tumour volume reported as 3mm (left-right), 5.4mm (cranio-caudal) and 4.5mm (anterior/ posterior). In terms of changes in tumour volume, Erridge *et al.* [33] showed that in a population of 25 patients, tumour shrinkage of at least 20% occurred in 40% of the patients. In Britton *et al.* [32], volume loss of at least 40% occurred in 50% of the patients. Bosmans *et al.* [26] report a 30% reduction in 13% of patients and a>30% increase in tumour size in 17% of patients. There are other reports of volumes increasing over the course of radiotherapy; for instance,Underberg *et al.* [34] reported an initial increase in tumour volume of 10cm^3 in at least 2 of 40 patients, however the incidence of increase in tumour volume does appear to be less than the incidence of tumour volume reduction. In order to identify and manage tumour migration, a 3-dimensional imaging technology is required at regular intervals over the course of treatment. This can be achieved with cone beam CT, 4D cone beam CT or a repeat 4D CT.

Set up (inter-fraction) error is a well-recognised problem that has been managed with offline MV images for many years [35]. With the addition of imaging capabilities on the treatment room, we are now able to perform online imaging to carry out a match and shift prior to treatment. The margin for set up errors is reduced with increased frequency of online set up, therefore daily online imaging offers the best chance of allowing dose escalation [36, 37]. This reduces the margins given for set up and therefore has the potential to allow dose escalation. Some studies have demonstrated that orthogonal kV images are equally good for online set up in every direction other than in rotation, where cone beam CT is superior [38]. However, due to the significant dose of a daily cone beam CT, it may be more appropriate to use kV orthogonal images when frequent imaging is required.

RESPIRATORY GATING

Respiratory Gated Radiotherapy (RGRT) involves treatment delivery at selected phases of the respiratory cycle. There are many commercial systems available; however, they all employ a surrogate to monitor the patient's respiration cycle. This surrogate is traced and enables the selection of a respiratory phase or "gate" for treatment delivery. The treatment beam is switched on only during this interval. RGRT can be delivered in end-inspiration or end-expiration but there is no consensus regarding the preferred phase [39]. End-inspiration captures the lung at maximum expansion therefore potentially sparing more normal lung tissue; however, the tumour remains in end-inspiration for significantly less time therefore there is a smaller treatment window. In addition, the end-inspiration tumour position is more variable than the end-expiration tumour position [40, 41]. In end-expiration, there is a longer treatment window, therefore the treatment is quicker and the tumour position is more stable. However, the lung is in a compressed state, therefore a greater volume of normal lung tissue will be contained within the treatment field and there is subsequently less sparing and less reduction in the volume of lung receiving predefined thresholds [24, 42]. RGRT can also be amplitude-based or phase-based. In amplitude-based gating, treatment delivery is based on the absolute position of the marker block on the

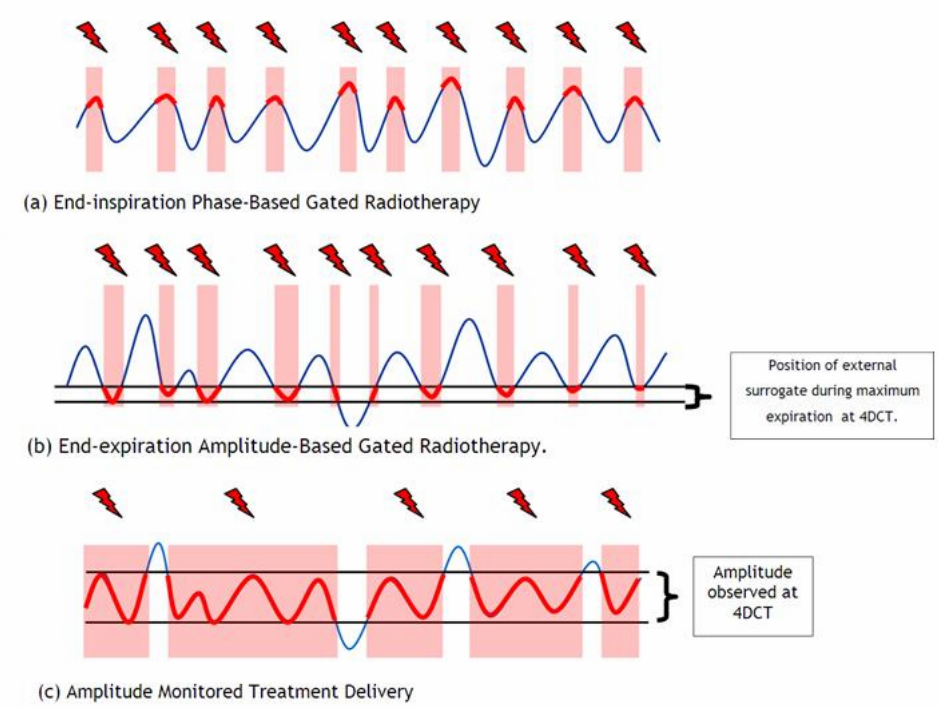

Figure 4 Different forms of respiratory gating.

patient's thorax or abdomen, regardless of the phases in the patient's respiratory cycle [42, 43]. In phase-based RGRT, the breathing cycle is divided into multiple time segments and radiation delivery is based on the same phase of the patient's respiratory cycle. This difference is illustrated in Figure 4. Dosimetric comparisons between the two methods have been performed and failed to find any significant difference in the dosimetric consequences of the two different forms of RGRT [42].

Spoelstra *et al*. [44] remains the sole publication confirming target coverage using RGRT. They demonstrated that with phase-gated RGRT in end-inspiration, the residual systematic (∑) and random (σ) errors in tumour position within the treatment "gate" were 1.8mm and 1.3mm medio-laterally and 1.7mm and 1.7mm cranio-caudally.

There are multiple volumetric and dosimetric studies looking at the potential benefits of RGRT. Wolthaus *et al*. [45] demonstrated that using RGRT, compared to conventional treatment, reduced PTV size by 11%. In comparing RGRT to a PTV incorporating all tumour motion, the PTV size reduced by around 15%. In addition there are a number of reports that demonstrated toxicity parameters are reduced [34, 42, 46]; however, there are concerns that despite excitement regarding the technique, the clinical benefit in larger, locally advanced tumours may not be sufficient to allow dose escalation as there is very limited reduction in toxicity parameters [24, 46]. Although there is a belief theoretically that the patients who will gain the most from RGRT can be selected on the basis of tumour motion, this has not been borne out in the literature [24, 46]. RGRT does offer a benefit in toxicity parameters in a small number of patients, with the potential to allow dose escalation, although these cannot be accurately predicted. To ensure there is clinical benefit to the patient, with all the extra time and potential errors that come with RGRT, a standard 4DCT plan should be calculated and compared to a RGRT plan to ensure RGRT offers an improved plan.

NOVEL PLANNING METHODS - INTENSITY MODULATED RADIOTHERAPY (IMRT)

Intensity modulated radiotherapy (IMRT) involves the use of multiple beams in which the beam intensity is modified across each beam. Each beam can only treat a portion of the target. IMRT can be planned by either forward or inverse planning.

It can be delivered through three main ways: "stop and shoot" where standard beams with fixed multi-leaf collimators (MLC) are used; dynamic IMRT where the beam is static although the MLCs are moving during the delivery; or intensity modulated arc therapy (IMAT) where the MLC, gantry and energy are all changing as the treatment is delivered.

There are several planning studies that have identified planning methods to potentially reduce toxicity to the oesophagus [47, 48] and the lung [49, 50]. Along with potential reduction of toxicity, there is potential for dose escalation with the promising aim of improved local control. However, due to the limited number of subjects involved, further work is required. For example, Grills *et al*. [51] performed a dosimetric study to assess the potential for dose escalation with IMRT. In node positive cases, when planning to identical normal-tissue constraints, IMRT was associated with mean target volume doses that were 25%-30% greater than those achieved with optimised 3D-conformal radiation,

confirming the role of IMRT as a potential means to achieve dose escalation.

Very few studies have reported on the clinical outcome of IMRT. Memorial Sloan Kettering has published its outcomes for 55 inoperable NSCLC patients treated with IMRT [52]. The 2-year local control (58%) and overall survival rates (58%) were encouraging for Stage III patients. However, these patients were treated with doses higher [mean prescription dose of 6950cGy (range 6000–9000 cGy)] than what would be perceived as standard. Without the comparison of a control arm, it is difficult to draw any definitive conclusions; however, it is a step forward in developing prospective studies in this area.

ADAPTIVE PLANNING

As discussed above, GTV can alter in size over the course of radiation treatment. Any enlargement in GTV or alteration in position or shape can be identified using 3D soft tissue online imaging and further planning scans can be performed to ensure the new position and size of the tumour is covered adequately throughout treatment. Conversely, if the tumour shrinks, this raises the possibility of reducing the GTV over the course of treatment which may offer the potential benefit of reducing normal tissue toxicity, thereby allowing dose escalation. This has been suggested by a few planning studies performed. Guckenberger *et al*. [53] demonstrated an average dose escalation from 67Gy to 74Gy and this was confirmed by Feng *et al*. [54] who reported doses of >80Gy were achieved in 5 out of 6 patients. However, there remains no clinical series of patients treated in this way. The primary concern is that although the GTV can visibly shrink on imaging, microscopic cancer cells (in particular radio-resistant stem cells) may remain in the now excluded areas at the periphery of target, which will compromise on the dose delivered to viable disease [55]. However, Guckenberger *et al*. [53] has recently performed a further planning study looking at tumour control probability with adaptive radiotherapy comparing static microscopic disease and shrinking microscopic disease. They found that adaptive planning did not compromise dose coverage of microscopic disease and contrary to the theory, improved tumour control probability by >40%. As a result of this study, we can perhaps look forward to clinical studies in this field [56].

ADVANCED IMAGING AND IMPROVEMENTS IN TNM STAGING

Accurate and reproducible tumour imaging plays a central role in the management of NSCLC. Over the past decade, with the advent of positron emission tomography (PET) and combined PET-CT scanning, our ability to more accurately determine TNM staging has significantly improved. Numerous studies correlating imaging with final pathological results [57–59] have now emerged, which demonstrate the superiority of hybrid functional and morphological imaging over conventional CT. It is not surprising that PET-CT is now accepted as an essential routine investigation especially if radical treatment is contemplated, for example in the recommendations by the Royal College of Radiologists, United Kingdom [60].

The approach of a hybrid or integrated PET-CT scanning has clear advantages over independent image acquisition followed by co-registration to produce composite images. With the latter, there are many potential sources of error at each step but it is very much centred around patient movement and the reproducibility of patient positioning [57, 61, 62]. Methods, such as fiducials, deformable registration or respiratory gating, to overcome co-registration have been developed [63]; however, an integrated image acquisition system remains preferable. In the authors' institution, integrated PET/CT scanning is used.

Two-[18F]-fluoro-2-deoxy-d-glucose or ^{18}FDG is by far the most commonly employed PET radiotracer which is relatively easy to produce and readily available. Suitability of ^{18}FDG is based on the principle of tumour glucose hyper-metabolism, the avidity of which has been linked to the rate of tumour growth [64]. Unlike other tracers which are also commercially available, ^{18}FDG's relatively longer half-life allows it to be transported from a remote cyclotron facility if none is available locally, another reason for its popularity. Details concerning the physical and biochemical properties of the various tracers available for functional imaging have already been reviewed as have the principles of image acquisition and interpretation [61, 65]. It is important to highlight that standardised and reproducible protocols are necessary as these influence image quality and, ultimately, the clinical conclusions drawn [57, 62]. Close attention has to be paid to technical factors such as half-life, amount of radiotracer delivered, uptake time, image acquisition time, attenuation correction, motion artefacts and clinical factors such as the size of lesions, presence of concurrent inflammatory or infective processes or the prevalence of physiological brown fat which may lead to false positive findings. Conversely, certain histological sub-types may demonstrate less intense FDG uptake such as well-differentiated adenocarcinoma [66, 67] and bronchoalveolar carcinoma [68] and this has to be carefully considered. The benefits of multidisciplinary team review, correlating clinical, radiological and pathological findings and auditing local experience cannot be underestimated [69, 70].

A pooled analysis of 378 patients estimates the accuracy of ^{18}FDG PET-CT in predicting T stage at around 82% with a 6% rate of overstaging and 13% rate of understaging [65] - this outperforms both CT or PET alone. Some authors, however, have shown only relatively modest gains delivered by PET-CT [71]. Greater gains have perhaps been more consistently demonstrated in the staging of more advanced tumours, namely T3 and T4 [72], and in determining the extent of chest wall and mediastinal invasion [73]. PET-CT also appears to be useful in detecting malignant pleural-based

metastases and effusions (with accuracies of between 84% and 92% [74, 75]) which according to the revised 7th AJCC/IUCC TNM staging nomenclature, constitutes metastatic disease and such patients would thus be unsuitable for radical radiotherapy. The relationship between maximum tumour SUV (SUV_{max}) and tumoural biology and prognosis has been extensively investigated. In a meta-analysis of 13 studies, Berghmans and colleagues [76] demonstrated that SUV was a significant prognostic factor for survival with a hazards ratio of 2.27. SUV_{max} has also been shown to correlate with histological sub-type [77] and grade [78]. However the clinical utility of SUV_{max} remains investigational.

Nodal assessment by ^{18}FDG PET-CT has had a major impact in the assessment of locally advanced NSCLC. Meta-analyses have demonstrated the superiority of functional imaging over CT assessment alone [79, 80], which is reliant on conventional interpretation based on size and, to a lesser extent, morphology. In a pooled analysis by De Wever and colleagues [65], the average sensitivity, specificity, positive predictive value (PPV), negative predictive value (NPV) and accuracy of PET-CT was found to be 73%, 80%, 78%, 91% and 87%, respectively. In the authors' institution, patients with PET-CT positive mediastinal nodal disease are routinely referred for histological confirmation [81]. False positive nodes caused by reactive inflammation and/or infection need to be discounted whereas discovery of advanced nodal disease precludes radical surgery. The issue of enlarged mediastinal nodes on CT but with negative on PET, is a more contentious issue. Due to a relatively high NPV reported across the literature [65, 79, 82] some argue that the incidence of micrometastatic disease is low and PET negative nodes do not have to be routinely sampled [81]. Others, such as the American College of Chest Physicians' guidelines, take the view that enlarged mediastinal lymphadenopathy should always be subject to histological clarification regardless whether the PET is positive or not [83], citing studies which have raised concerns over the issue of false negatives [84, 85].

Another utility of PET-CT is in uncovering occult distant metastases, see Figure 5. The rate varies, but in one study the incorporation of functional imaging into the diagnostic process precluded radical treatment in as many as 25% of patients [86], hence demonstrating a significant clinical impact. The introduction of integrated PET-CT has been useful in clarifying distant lesions such as those in the adrenal glands and bones, which have previously been equivocal based on size criteria alone. Given that radical regimes for locally advanced NSCLC are invariably intensive, careful selection of patients is crucial to avoid potentially significant morbidity in those who are unlikely to benefit [87].

NON-RIGID IMAGE REGISTRATION

Modern hybrid PET-CT scanners employ automatic rigid-body image registration algorithms to fuse the pairs of image data sets. As mentioned above, PET and CT images are acquired over significantly different time-scales. Even with automatic registration, alignment errors occur, and can lead to artefacts in SUV, tumour volumes and position. In fact, there are reports of up to 96% of combined PET-CT scans showing respiratory motion artefacts, with target registration errors of up to 11 mm [88]. Further, it is known that the lungs suffer deformations due to respiration, gravity and acceleration of body force [89]. Solutions will generally be to acquire each image set with respiratory correlation techniques, and to register employing alternate registration algorithms, such as non-rigid techniques [90].

Some early reports demonstrated the promise of these techniques, but processing times were long (45–75 mins for data from combined or separate PET and CT scanners, respectively) [88]. In 2007, Orban de Xirvy *et al*. [91] assessed the benefit of deformable registration for 4D CT data. In fact, they found that differences in tumour delineation between rigid and non-rigid registration datasets were similar to inter-observer variability.

Grgic *et al*. [92] have reported results of a comparison between rigid and non-rigid registration of PET-CT images for a group of 16 lung cancer patients. Registrations were performed for scans acquired at expiration, inspiration and mid-cycle respiration. Registration accuracy measurements were based on

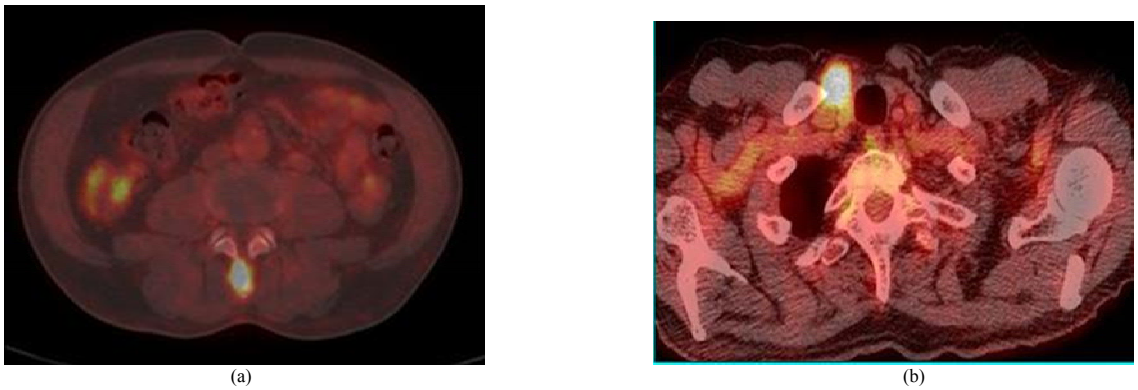

(a) (b)

Figure 5 PET-CT Improves TNM Staging of Non-Small Cell Lung Carcinoma. Occult metastases from NSCLC uncovered by PET-CT as part of the staging protocol prior to radical treatment. a) metastases in the spinous process of vertebrae. b) metastases in a contralateral supraclavicular fossa lymph node.

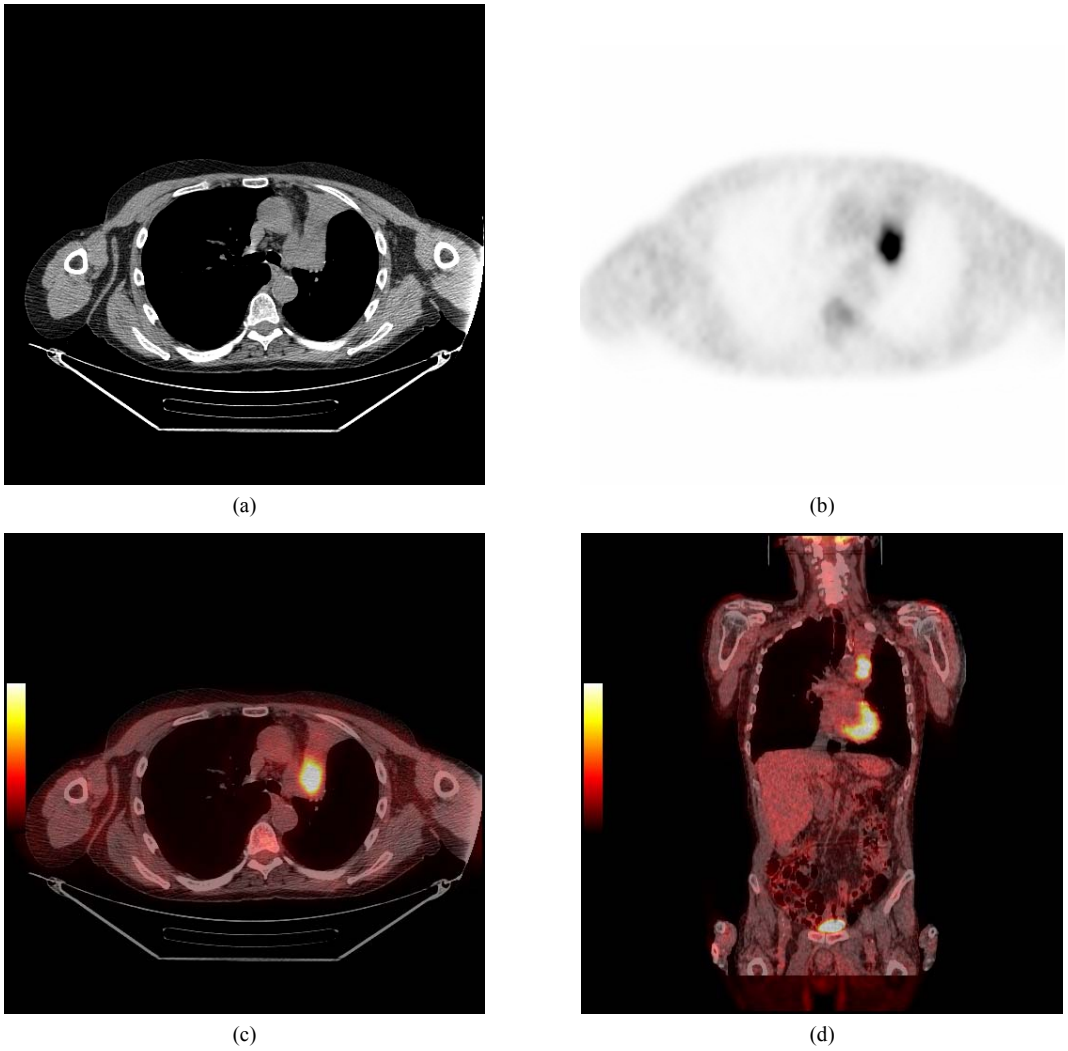

Figure 6 PET-CT Improves Target Volume Definition for Radical Radiotherapy. A series of CT, PET and fused CT-PET images of a left upper lobe primary NSCLC. a) Axial CT image, this highlights the difficulty in differentiating tumour from atelectasis and/or collapse/consolidation of normal lung. b) Axial PET image shows area of intense ^{18}FDG uptake corresponding to tumour but the image lacks anatomical definition. c) Axial PET-CT fusion image clearly improves the clinicians ability to localise tumour for purposes of GTV definition. d) Coronal PET-CT image of the same tumour.

observer scoring of landmarks. The non-rigid registrations showed modest improvements in alignment for the extremes of respiration, but not for mid-breathing.

Current algorithms, encompassing finite element analysis and biomechanical-based registration, offer solutions with high accuracy [93]. It should be noted that for tumour tracing, some reports have shown that the lung tumours do not deform significantly [94]. They mainly translate, such that rigid-body image registration is sufficient. The overall benefit of non-rigid registration seems modest, and work remains to be done to improve inter-observer error rates.

THE USE OF ADVANCED IMAGING IN RADIOTHERAPY PLANNING

Advances in imaging are also changing the way radiation oncologists undertake treatment planning [57, 61]. Despite well-described protocols for diagnosis, the methodologies for the optimal use of PET-CT in radiation planning remains complex and, as yet, not standardised [57]. Moreover, evidence demonstrating improved patient outcomes over and above CT-based planning remains limited [95]. It is interesting to reflect that many of the techniques which we would now consider as standard, such the use of CT planning in 3D conformal radiotherapy, have been widely adopted in the past without randomised evidence [96].

Studies have demonstrated that PET-CT based radiotherapy planning improves accuracy and alters target volume definition [97–99]. One study has demonstrated that PET-CT reduced geographical miss or underdosing in up to 40% of patients [51]. PET-CT seems to be particularly valuable in differentiating between collapse/consolidation and/or distal lung atelectasis versus tumour [99] which is often hard to differentiate on CT (see Figure 6). It has been shown that in the absence of PET-CT, clinicians tend to overestimate GTV and CTV, erring on the side of caution so as not to produce geographical miss [99]. Tighter GTV definition has a corollary effect at reducing OAR (organ at risk) dose, for example dose to spinal cord [97]. As discussed above, PET-CT is beneficial in

assessing mediastinal lymph nodes [100]. This is particularly relevant in locally advanced tumours where primary tumour radiotherapy volumes already tend to be sizeable and inclusion of geographically separate involved nodal regions as GTV can increase irradiated volumes significantly. Finally, inter-observer variability in outlining GTV is a well-described phenomenon in lung cancer radiotherapy [101] despite the use of well-defined institutional protocols for conformal CT-based planning [102]. The use of PET-CT has been shown to reduce this variability, producing tighter GTV concordance [103, 104], independent of diagnostic upstaging or downstaging of the actual disease.

In order to facilitate compatibility between images acquired in the PET-CT suite for radiation planning, the patient would ideally be positioned on a rigid couch top, in the treatment position, using the same set-up parameters and immobilisation device. The aperture will need to be wide-bore to accommodate the additional equipment. The use of lasers for patient alignment is recommended and the scanning process should be undertaken under the supervision of the therapy radiographer. The software will need to be compatible between the imaging and radiotherapy planning systems with care taken over the integrity of data transfer. Essentially imaging should be considered a crucial link in the chain of radiotherapy quality assurance and we refer the reader to publications that discuss these issues further [57, 105, 106].

When viewing acquired images, the physician has to be aware of several differences between conventional CT and PET-CT. PET images are acquired over several respiratory cycles and the result is a blurred effect at the edges. The SUV outputs are influenced by avidity of uptake, size of the lesion and tumour biology. Image clarity can be significantly influenced by display settings such as contrast and grey/colour scale and other factors such as attenuation correction. These technical considerations pose a new challenge for the radiation oncologist. It is crucial to fully review the clinico-pathological details of the patients carefully and obtain input by the nuclear medicine physician or radiologist with interest in PET-CT particularly in the steep learning phase of adopting this technology.

Various efforts to standardise GTV definition remain ongoing [57]. No one method can be recommended for routine clinical practice as borne out by a recent International Atomic Energy Agency (IAEA) report [57]. Currently, the majority of departments use visual interpretation, delineating the CT volume associated with the visually identified lesion on PET-CT [107]. This does rely on the experience of the operator in correlating PET-CT images with clinical and anatomical data, coupled with knowledge of the technical factors involved in image acquisition and display.

Alternative methods include a semi- or fully-automated segmentation approach with thresholds based on quantitative thresholds such as SUV. In some studies, an absolute value of SUV=2.5 has been taken to differentiate benign and malignant tissue. This has then been used by some centres in delineating GTV, for example Paulino *et al.* [108]. Other studies have contoured GTV as percentage of SUV_{max}, using values ranging from 15–50%, though 40% is now commonly used [109, 110]. Biehl *et al.* [111] performed a prospective study of 19 patients to assess the impact of using percentage SUV_{max} thresholds of 20% versus 40% on GTV volume. Thresholds were also adjusted to obtain 1:1 match of PET-based and CT-based GTV volumes. They found that the optimal threshold varied with tumour size, and one single threshold was not accurate. Their study does, of course, assume that the CT-based GTV is 'true', when pathological validation would be preferred. A point to note is that SUV_{max} can vary widely depending on histological sub-type [77] and grade [78]. Moreover, non-malignant areas such as inflammation or infection can also demonstrate a high SUV. An example of the different qualitative and quantitative methods of PET-CT voluming is shown in Figure 7.

More complex algorithms have also been suggested [112, 113]. Rather than using crude absolute thresholding, or one based on a percentage of region point maximum, they have based algorithms on (mean) source to background ratios. To achieve the true threshold volume, Black *et al.* [112] noted a linear relationship between mean target SUV and the threshold SUV required, i.e. again, no global or single threshold was found to be appropriate. In phantom data comparisons, they found their algorithm performed well, yielding approximately 1% deviations from true volumes, compared to mean

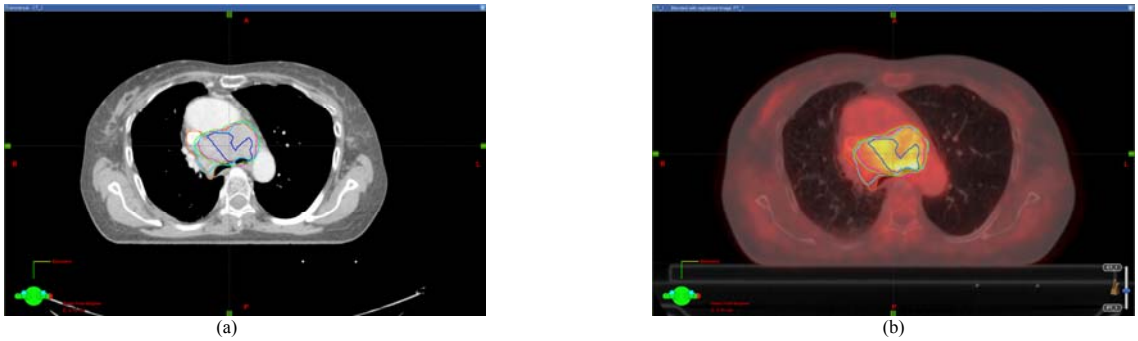

(a) (b)

Figure 7 PET-CT Assisted Target Volume Definition. This figure shows the differences in GTV contours produced using different qualitative and quantitative voluming methods on the axial same slice (orange is CT only, light blue is PET assisted qualitative visual mark-up, cyan SUV 2.5, green is 40% of SUVmax, dark blue is 60% of SUVmax). The additional information provided by PET-CT is graphically illustrated when a) CT alone is compared to b) blended CT and PET-CT. Additional volumes such as 60% of SUVmax can be generated which may have implications when moving towards selective regional dose escalation or dose painting.

deviations of 23% for constant threshold methods. Variation in target volumes and background levels were found to have minimal impact. Certainly, use of thresholds based on mean target intensities seem preferable to those based on percentage maximum values; however, an iterative process is necessary to define a threshold contour in which to calculate the mean intensity. Black *et al*. [112] also highlighted significant limitations with their algorithm - they noted problems under circumstances where the target exhibited significantly heterogeneous activity, where the target was in a region of high background (e.g. mediastinum), or where mean SUV was low (<2.0), which can lead to significant errors. Dasine *et al*. [113] also demonstrated success with a similar regression algorithm for thresholding. They also noted a dependence on the particular algorithm used for PET image reconstruction. In pathological validation, PET delineated volumes proved to be more accurate than MRI and CT.

Nestle *et al*. [114] performed a study of 25 NSCLC patients, comparing 4 delineation methods. The methods included visual use of PET information, thresholding with 40% of SUV_{max}, absolute SUV=2.5, and a signal to background method, where mean target is based on 70% SUV_{max}. The CT volumes, based on 3D rather than 4D scans, were used for validation, but volumes were expanded to account for motion, using realistic margins. They found that visual determination and use of SUV=2.5 generated similar results, but over-estimated the target volumes compared to expanded CT volumes. The 40% SUV_{max} method appeared to generate the largest volume errors, especially for heterogenous targets. Their signal to background algorithm seems to generate results with errors between those of SUV=2.5 and 40% SUV_{max}. It appears that the definition of relevant background was not simple.

In 2007, van Baardeijk *et al*. [58] performed a study of tumour auto-contouring, based on a ratio of source to background. The study, involving 33 patients with histologically proven NSCLC, showed a strong correlation (Pearsons correlation coefficient 0.9) between pathological tumour size and that for auto-thresholding. The sensitivity and specificity of the technique were also improved compared to the usual reports from the Nuclear Medicine department.

Therefore, as with all emerging technologies, it is essential to continue to audit patient outcomes, including carefully documenting patterns of local failure. Whenever semi or automated volumes are generated, the final step should always include physician review with contour editing as appropriate.

4D PET-CT

As a medical imaging modality, PET image acquisition is comparatively slow, with a typical half-body lung scan taking 30–40 mins. During free-breathing, acquisition takes place over many respiratory cycles, resulting in images which display motional blurring. The entirety of tumour excursion is shown, and the tumour representation can be compared to that of slow CT [115], or the average-IP of 4DCT. This can pose challenges for strategies designed to reduce radiotherapy margins and dose escalation.

The presence of tumour motion in images has several well-known consequences. Tumour volumes can be over-estimated. Artefacts in SUV can occur, leading to an underestimation of SUV_{max} for a region. Blurring due to respiratory motion will also reduce the measured activity per voxel in the tumour – which will also affect the tumour contrast in the PET image and affect the SUV generated. This in turn can lead to dosimetric errors in planning (under- and over-dosing). CT acquisition is significantly faster than PET. The mismatch in CT and PET images can then lead to attenuation correction errors, registration errors and associated tumour positional errors [116–118].

Like motion-correlated CT acquisition methods, 4D PET-CT is an attractive solution for gating and margin-reduced treatment [116]. This method uses similar motion surrogates, allowing acquisition of motion correlated images during the respiration, which can be binned based on amplitude or phase. Phantom methods have shown improved measurement of lesion volume and SUV [119, 120]. In a small study of 5 lung cancer patients, Nehmeh *et al*. [116] demonstrated tumour volume reduction (between 13.8% and 34.6%) when using gated 4D PET-CT compared to ungated acquisition. This decrease in volume was accompanied by an increase in signal per voxel in the tumour and SUV_{max}. Scores for total lesion gylcolysis, TLG, (defined as the product of SUVmax x lesion volume) were well correlated for gated and ungated PET acquisitions. Although there is much potential, clinical implementation of 4D PET has been slow, and the technique continues to pose technical challenges, due to increased image noise compared to static PET, and uncertainties due to image mismatch issues [117].

MRI TECHNIQUES : 4D MRI

For many tumour types, MRI represents the modality of choice due to its superior soft tissue imaging ability [121]. For many years, MRI has had the capability of high temporal rate imaging, with image acquisition within 10s of milliseconds, offering benefit for cardiac imaging, for example [122]. Already some groups have reported the benefit of using dynamic MRI to assess lung motion [123, 124]. A natural extension would be to attempt respiratory-correlated imaging, thereby rivalling 4D CT.

Remmert *et al*. [125] presented an early report on the feasibility of 4D MRI. They implemented the technique, based on retrospective sorting of standard 2D-FLASH MR images, on a dynamic phantom. The image sorting was based on the motion of an external surrogate but controversially this was mounted on the pump, not on the anatomy phantom. An artificial contrast agent gel was also injected into the lungs of the phantom. Motion demonstrated on the 4D images correlated well with that

programmed by the phantom, with uncertainty in the order of 1mm. In a more recent study, Biederer *et al*. [126] compared motional correlation methods using 4D CT, MRI and 4D cone beam CT, also based on a porcine phantom. They found 4D MR and 4D cone beam CT over-estimated lesion volumes compared to static and dynamic CT. Inter-observer correlation was also poorer for 4D MR and cone beam CT. Undoubtedly, interest in 4D MR methods will continue to increase.

MRI TECHNIQUES : MRI USING HYPERPOLARISED NOBLE GASES

Conventional proton MRI struggles to achieve high quality images of the lung. Image signal to noise in lung is poor due to low spin densities, and large differences in tissue susceptibility. However, over the last decade, MRI involving the use of hyperpolarised noble gases (e.g. helium and xenon) has enabled high quality quantitative images of pulmonary function [127]. These images, visually similar to those using radionuclides, only show the regional presence of the hyperpolarised gas, without any surrounding anatomy. Registration of these images with standard morphological proton MRI is therefore highly beneficial.

Whilst most users have focussed on non-malignant medical conditions such as COPD [128], some groups have assessed the potential impact of these functional lung images for radiotherapy. Functional imaging with helium-3 (He-3) MRI offers the potential to differentiate between viable, and non-viable tissue, allowing plans to be optimised, to direct beam portals through regions already compromised, and avoid viable lung tissue. In 2007, Ireland *et al*. [129] demonstrated the feasibility of generating functionally-weighted IMRT plans with the use of hyperpolarised MRI images, for 6 NSCLC patients. The use of He-3 MR images in plan optimisation enabled a small, but statistically significant, reduction in V20, not just for the well ventilated lung, but also for the total lung volume. Allen *et al*. [130] acquired hyperpolarised He-3 MR images before and after radiotherapy for NSCLC patients. Varied results were found, with He-3 MR showing poor correlation with CT and PET volumes before and after radiotherapy. A larger variation in changes relating to response to radiotherapy was also demonstrated by the He-3 images.

MRI using hyperpolarised gases certainly shows modest potential for use in radiotherapy planning, but considerably more work is required for convincing benefit. Similarly, work also remains to be done in demonstrating the potential for staging and treatment response. This is hampered by worldwide shortages of helium gas and significantly increasing prices. It may be that future studies must be directed to exploring the use of other noble gases such as xenon.

CONCLUSION

There continues to be ongoing challenges in the delivery of radical radiotherapy in locally advanced non-small cell lung cancer. These challenges are currently being addressed in a number of ways. Advanced imaging techniques have the potential to improve TNM staging and target volume definition. Improvements in planning methods and on-board imaging technology have the potential to improve both intra- and inter-fraction motion management. Despite this, there remains much to be done in order to optimise the delivery of radical radiotherapy for this group of patients. It is hoped that better technical expertise will eventually lead to improved clinical outcomes.

ACKNOWLEDGEMENTS

The authors would like to acknowledge the assistance provided by Kim Bloomer, Sebeena Sidhu, Marimuthu Sankaralingam and Stefano Schipani of the Beatson West of Scotland Cancer Centre, United Kingdom in preparing the images for this article.

REFERENCES

1. Detterbeck FC, Boffa DJ and Tanoue LT. The new lung cancer staging system. Chest 2009; 136(1):260–271.
2. Rami-Porta R, Crowley JJ and Goldstraw P. The revised TNM staging system for lung cancer. Ann Thorac Cardiovasc Surg 2009; 15(1):4–9.
3. Goldstraw P, Ball D, Jett JR, Le Chevalier T, Lim E, Nicholson AG and Shepherd FA. Non-small-cell lung cancer. Lancet 2011; 378(9804):1727–1740.
4. De Ruysscher D, Faivre-Finn C, Nestle U, Hurkmans CW, Le Péchoux C, Price A and Senan S. European Organisation for Research and Treatment of Cancer recommendations for planning and delivery of high-dose, high-precision radiotherapy for lung cancer. J Clin Oncol 2010; 28(36):5301–5310.
5. Nakayama H, Satoh H, Kurishima K, Ishikawa H and Tokuuye K. High-dose conformal radiotherapy for patients with stage III non-small-cell lung carcinoma. Int J Radiat Oncol Biol Phys 2010; 78(3):645–650.
6. Daisne JF and Grégoire V. [Multimodalities imaging for target volume definition in radiotherapy]. Bull Cancer 2006; 93(12):1175–1182.
7. Steenbakkers RJ, Duppen JC, Fitton I, Deurloo KE, Zijp LJ, Comans EF, Uitterhoeve AL, Rodrigus PT, Kramer GW, Bussink J, De Jaeger K, Belderbos JS, Nowak PJ, van Herk M and Rasch CR. Reduction of observer variation using matched CT-PET for lung cancer delineation: a three-dimensional analysis. Int J Radiat Oncol Biol Phys 2006; 64(2):435–448.
8. Vorwerk H, Beckmann G, Bremer M, Degen M, Dietl B, Fietkau R, Gsänger T, Hermann RM, Alfred Herrmann MK, Höller U, van Kampen M, Körber W, Maier B, Martin T, Metz M, Richter R, Siekmeyer B, Steder M, Wagner D, Hess CF, Weiss E and Christiansen H. The delineation of target volumes for radiotherapy of lung cancer patients. Radiother Oncol 2009; 91(3):455–460.
9. Stevens CW, Munden RF, Forster KM, Kelly JF, Liao Z, Starkschall G, Tucker S and Komaki R. Respiratory-driven lung tumor motion is independent of tumor size, tumor location, and pulmonary function. Int J Radiat Oncol Biol Phys 2001; 51(1):62–68.
10. van Sörnsen de Koste JR, Lagerwaard FJ, Nijssen-Visser MR, Graveland WJ and Senan S. Tumor location cannot predict the mobility of lung tumors: a 3D analysis of data generated from multiple CT scans. Int J Radiat Oncol Biol Phys 2003; 56(2):348–354.
11. Liu HH, Balter P, Tutt T, Choi B, Zhang J, Wang C, Chi M, Luo D, Pan T, Hunjan S, Starkschall G, Rosen I, Prado K, Liao Z, Chang J,

Komaki R, Cox JD, Mohan R and Dong L. Assessing respiration-induced tumor motion and internal target volume using four-dimensional computed tomography for radiotherapy of lung cancer. Int J Radiat Oncol Biol Phys 2007; 68(2):531–540.

12. Pantarotto JR, Piet AH, Vincent A, van Sörnsen de Koste JR and Senan S. Motion analysis of 100 mediastinal lymph nodes: potential pitfalls in treatment planning and adaptive strategies. Int J Radiat Oncol Biol Phys 2009; 74(4):1092–1099.
13. Bosmans G, van Baardwijk A, Dekker A, Ollers M, Wanders S, Boersma L, Lambin P and De Ruysscher D. Time trends in nodal volumes and motion during radiotherapy for patients with stage III non-small-cell lung cancer. Int J Radiat Oncol Biol Phys 2008; 71(1):139–144.
14. van der Geld YG, Senan S, van Sörnsen de Koste JR, van Tinteren H, Slotman BJ, Underberg RW and Lagerwaard FJ. Evaluating mobility for radiotherapy planning of lung tumors: a comparison of virtual fluoroscopy and 4DCT. Lung Cancer 2006; 53(1):31–37.
15. Underberg RW, Lagerwaard FJ, Cuijpers JP, Slotman BJ, van Sörnsen de Koste JR and Senan S. Four-dimensional CT scans for treatment planning in stereotactic radiotherapy for stage I lung cancer. Int J Radiat Oncol Biol Phys 2004; 60(4):1283–1290.
16. Rietzel E, Liu AK, Doppke KP, Wolfgang JA, Chen AB, Chen GT and Choi NC. Design of 4D treatment planning target volumes. Int J Radiat Oncol Biol Phys 2006; 66(1):287–295.
17. Muirhead R, McNee SG, Featherstone C, Moore K and Muscat S. Use of Maximum Intensity Projections (MIPs) for target outlining in 4DCT radiotherapy planning. J Thorac Oncol 2008; 3(12):1433–1438.
18. Michalski D, Sontag M, Li F, de Andrade RS, Uslene I, Brandner ED, Heron DE, Yue N and Huq MS. Four-dimensional computed tomography-based interfractional reproducibility study of lung tumor intrafractional motion. Int J Radiat Oncol Biol Phys 2008; 71(3):714–724.
19. Guckenberger M, Wilbert J, Meyer J, Baier K, Richter A and Flentje M. Is a single respiratory correlated 4D-CT study sufficient for evaluation of breathing motion? Int J Radiat Oncol Biol Phys 2007; 67(5):1352–1359.
20. Kong FM, Hayman JA, Griffith KA, Kalemkerian GP, Arenberg D, Lyons S, Turrisi A, Lichter A, Fraass B, Eisbruch A, Lawrence TS and Ten Haken RK. Final toxicity results of a radiation-dose escalation study in patients with non-small-cell lung cancer (NSCLC): predictors for radiation pneumonitis and fibrosis. Int J Radiat Oncol Biol Phys 2006; 65(4):1075–1086.
21. Bradley J, Graham MV, Winter K, Purdy JA, Komaki R, Roa WH, Ryu JK, Bosch W and Emami B. Toxicity and outcome results of RTOG 9311: a phase I-II dose-escalation study using three-dimensional conformal radiotherapy in patients with inoperable non-small-cell lung carcinoma. Int J Radiat Oncol Biol Phys 2005; 61(2):318–328.
22. Belderbos JS, De Jaeger K, Heemsbergen WD, Seppenwoolde Y, Baas P, Boersma LJ and Lebesque JV. First results of a phase I/II dose escalation trial in non-small cell lung cancer using three-dimensional conformal radiotherapy. Radiother Oncol 2003; 66(2):119–126.
23. Partridge M, Ramos M, Sardaro A and Brada M. Dose escalation for non-small cell lung cancer: analysis and modelling of published literature. Radiother Oncol 2011; 99(1):6–11.
24. Muirhead R, Featherstone C, Duffton A, Moore K and McNee S. The potential clinical benefit of respiratory gated radiotherapy (RGRT) in non-small cell lung cancer (NSCLC). Radiother Oncol 2010; 95(2):172–177.
25. Chang JY, Dong L, Liu H, Starkschall G, Balter P, Mohan R, Liao Z, Cox JD and Komaki R. Image-guided radiation therapy for non-small cell lung cancer. J Thorac Oncol 2008; 3(2):177–186.
26. Bosmans G, van Baardwijk A, Dekker A, Ollers M, Boersma L, Minken A, Lambin P and De Ruysscher D. Intra-patient variability of tumor volume and tumor motion during conventionally fractionated radiotherapy for locally advanced non-small-cell lung cancer: a prospective clinical study. Int J Radiat Oncol Biol Phys 2006; 66(3):748–753.
27. Sonke JJ, Lebesque J and van Herk M. Variability of four-dimensional computed tomography patient models. Int J Radiat Oncol Biol Phys 2008; 70(2):590–598.
28. Poulsen PR, Cho B and Keall PJ. A method to estimate mean position, motion magnitude, motion correlation, and trajectory of a tumor from cone-beam CT projections for image-guided radiotherapy. Int J Radiat Oncol Biol Phys 2008; 72(5):1587–1596.
29. Sonke JJ, Rossi M, Wolthaus J, van Herk M, Damen E and Belderbos J. Frameless stereotactic body radiotherapy for lung cancer using four-dimensional cone beam CT guidance. Int J Radiat Oncol Biol Phys 2009; 74(2):567–574.
30. Muirhead R, van der Weide L, van Sornsen de Koste JR, Cover KS and Senan S. Use of megavoltage cine-images for studying intra-thoracic motion during radiotherapy for locally advanced lung cancer. Radiother Oncol 2011; 99(2):155–160.
31. Sixel KE, Ruschin M, Tirona R and Cheung PC. Digital fluoroscopy to quantify lung tumor motion: potential for patient-specific planning target volumes. Int J Radiat Oncol Biol Phys 2003; 57(3):717–723.
32. Britton KR, Starkschall G, Tucker SL, Pan T, Nelson C, Chang JY, Cox JD, Mohan R and Komaki R. Assessment of gross tumor volume regression and motion changes during radiotherapy for non-small-cell lung cancer as measured by four-dimensional computed tomography. Int J Radiat Oncol Biol Phys 2007; 68(4):1036–1046.
33. Erridge SC, Seppenwoolde Y, Muller SH, van Herk M, De Jaeger K, Belderbos JS, Boersma LJ and Lebesque JV. Portal imaging to assess set-up errors, tumor motion and tumor shrinkage during conformal radiotherapy of non-small cell lung cancer. Radiother Oncol 2003; 66(1):75–85.
34. Underberg RW, van Sörnsen de Koste JR, Lagerwaard FJ, Vincent A, Slotman BJ and Senan S. A dosimetric analysis of respiration-gated radiotherapy in patients with stage III lung cancer. Radiat Oncol 2006; 1:8.
35. Valicenti RK, Michalski JM, Bosch WR, Gerber R, Graham MV, Cheng A, Purdy JA and Perez CA. Is weekly port filming adequate for verifying patient position in modern radiation therapy? Int J Radiat Oncol Biol Phys 1994; 30(2):431–438.
36. Bel A, van Herk M, Bartelink H and Lebesque JV. A verification procedure to improve patient set-up accuracy using portal images. Radiother Oncol 1993; 29(2):253–260.
37. Higgins J, Bezjak A, Hope A, Panzarella T, Li W, Cho JB, Craig T, Brade A, Sun A and Bissonnette JP. Effect of image-guidance frequency on geometric accuracy and setup margins in radiotherapy for locally advanced lung cancer. Int J Radiat Oncol Biol Phys 2011; 80(5):1330–1337.
38. Li H, Zhu XR, Zhang L, Dong L, Tung S, Ahamad A, Chao KS, Morrison WH, Rosenthal DI, Schwartz DL, Mohan R and Garden AS. Comparison of 2D radiographic images and 3D cone beam computed tomography for positioning head-and-neck radiotherapy patients. Int J Radiat Oncol Biol Phys 2008; 71(3):916–925.
39. Biancia CD, Yorke E, Chui CS, Giraud P, Rosenzweig K, Amols H, Ling C and Mageras GS. Comparison of end normal inspiration and expiration for gated intensity modulated radiation therapy (IMRT) of lung cancer. Radiother Oncol 2005; 75(2):149–156.
40. Barnes EA, Murray BR, Robinson DM, Underwood LJ, Hanson J and Roa WH. Dosimetric evaluation of lung tumor immobilization using breath hold at deep inspiration. Int J Radiat Oncol Biol Phys 2001; 50(4):1091–1098.
41. Nakagawa K, Aoki Y, Akanuma A, Onogi Y, Terahara A, Sakata K, Muta N, Sasaki Y, Kawakami H and Hanakawa K. Real-time beam monitoring in dynamic conformation therapy. Int J Radiat Oncol Biol Phys 1994; 30(5):1233–1238.
42. Saito T, Sakamoto T and Oya N. Comparison of gating around end-expiration and end-inspiration in radiotherapy for lung cancer. Radiother Oncol 2009; 93(3):430–435.
43. Giraud P, Yorke E, Ford EC, Wagman R, Mageras GS, Amols H, Ling CC and Rosenzweig KE. Reduction of organ motion in lung tumors with respiratory gating. Lung Cancer 2006; 51(1):41–51.
44. Spoelstra FO, van Sörnsen de Koste JR, Cuijpers JP, Lagerwaard FJ, Slotman BJ and Senan S. Analysis of reproducibility of respiration-triggered gated radiotherapy for lung tumors. Radiother Oncol 2008; 87(1):59–64.
45. Wolthaus JW, Sonke JJ, van Herk M, Belderbos JS, Rossi MM, Lebesque JV and Damen EM. Comparison of different strategies to use four-dimensional computed tomography in treatment planning for lung cancer patients. Int J Radiat Oncol Biol Phys 2008; 70(4):1229–1238.
46. Starkschall G, Forster KM, Kitamura K, Cardenas A, Tucker SL and Stevens CW. Correlation of gross tumor volume excursion with potential benefits of respiratory gating. Int J Radiat Oncol Biol Phys 2004; 60(4):1291–1297.

47. Xiao Y, Werner-Wasik M, Michalski D, Houser C, Bednarz G, Curran W and Galvin J. Comparison of three IMRT inverse planning techniques that allow for partial esophagus sparing in patients receiving thoracic radiation therapy for lung cancer. Med Dosim 2004; 29(3):210–216.
48. Chapet O, Thomas E, Kessler ML, Fraass BA and Ten Haken RK. Esophagus sparing with IMRT in lung tumor irradiation: an EUD-based optimization technique. Int J Radiat Oncol Biol Phys 2005; 63(1):179–187.
49. Lavrenkov K, Singh S, Christian JA, Partridge M, Nioutsikou E, Cook G, Bedford JL and Brada M. Effective avoidance of a functional spect-perfused lung using intensity modulated radiotherapy (IMRT) for non-small cell lung cancer (NSCLC): an update of a planning study. Radiother Oncol 2009; 91(3):349–352.
50. Chapet O, Fraass BA and Ten Haken RK. Multiple fields may offer better esophagus sparing without increased probability of lung toxicity in optimized IMRT of lung tumors. Int J Radiat Oncol Biol Phys 2006; 65(1):255–265.
51. Grills IS, Yan D, Black QC, Wong CY, Martinez AA and Kestin LL. Clinical implications of defining the gross tumor volume with combination of CT and 18FDG-positron emission tomography in non-small-cell lung cancer. Int J Radiat Oncol Biol Phys 2007; 67(3):709–719.
52. Sura S, Gupta V, Yorke E, Jackson A, Amols H and Rosenzweig KE. Intensity-modulated radiation therapy (IMRT) for inoperable non-small cell lung cancer: the Memorial Sloan-Kettering Cancer Center (MSKCC) experience. Radiother Oncol 2008; 87(1):17–23.
53. Guckenberger M, Wilbert J, Richter A, Baier K and Flentje M. Potential of adaptive radiotherapy to escalate the radiation dose in combined radiochemotherapy for locally advanced non-small cell lung cancer. Int J Radiat Oncol Biol Phys 2011; 79(3):901–908.
54. Feng M, Kong FM, Gross M, Fernando S, Hayman JA and Ten Haken RK. Using fluorodeoxyglucose positron emission tomography to assess tumor volume during radiotherapy for non-small-cell lung cancer and its potential impact on adaptive dose escalation and normal tissue sparing. Int J Radiat Oncol Biol Phys 2009; 73(4):1228–1234.
55. Sonke JJ and Belderbos J. Adaptive radiotherapy for lung cancer. Semin Radiat Oncol 2010; 20(2):94–106.
56. Gomez DR and Chang JY. Adaptive radiation for lung cancer. J Oncol 2011; 2011:898391.
57. MacManus M, Nestle U, Rosenzweig KE, Carrio I, Messa C, Belohlavek O, Danna M, Inoue T, Deniaud-Alexandre E, Schipani S, Watanabe N, Dondi M and Jeremic B. Use of PET and PET/CT for radiation therapy planning: IAEA expert report 2006-2007. Radiother Oncol 2009; 91(1):85–94.
58. van Baardwijk A, Bosmans G, Boersma L, Buijsen J, Wanders S, Hochstenbag M, van Suylen RJ, Dekker A, Dehing-Oberije C, Houben R, Bentzen SM, van Kroonenburgh M, Lambin P and De Ruysscher D. PET-CT-based auto-contouring in non-small-cell lung cancer correlates with pathology and reduces interobserver variability in the delineation of the primary tumor and involved nodal volumes. Int J Radiat Oncol Biol Phys 2007; 68(3):771–778.
59. Faria SL, Menard S, Devic S, Sirois C, Souhami L, Lisbona R and Freeman CR. Impact of FDG-PET/CT on radiotherapy volume delineation in non-small-cell lung cancer and correlation of imaging stage with pathologic findings. Int J Radiat Oncol Biol Phys 2008; 70(4):1035–1038.
60. The Royal College of Radiologists. Indications for PET-CT: Guidance from the Royal College of Radiologists. London: The Royal College of Radiologists, 2010.
61. Aristei C, Falcinelli L, Palumbo B and Tarducci R. PET and PET-CT in radiation treatment planning for lung cancer. Expert Rev Anticancer Ther 2010; 10(4):571–584.
62. Westerterp M, Pruim J, Oyen W, Hoekstra O, Paans A, Visser E, van Lanschot J, Sloof G and Boellaard R. Quantification of FDG PET studies using standardised uptake values in multi-centre trials: effects of image reconstruction, resolution and ROI definition parameters. Eur J Nucl Med Mol Imaging 2007; 34(3):392–404.
63. Goerres GW, Kamel E, Seifert B, Burger C, Buck A, Hany TF and Von Schulthess GK. Accuracy of image coregistration of pulmonary lesions in patients with non-small cell lung cancer using an integrated PET/CT system. J Nucl Med 2002; 43(11):1469–1475.
64. Duhaylongsod FG, Lowe VJ, Patz EF Jr, Vaughn AL, Coleman RE and Wolfe WG. Lung tumor growth correlates with glucose metabolism measured by fluoride-18 fluorodeoxyglucose positron emission tomography. Ann Thorac Surg 1995; 60(5):1348–1352.
65. De Wever W, Stroobants S, Coolen J and Verschakelen JA. Integrated PET/CT in the staging of nonsmall cell lung cancer: technical aspects and clinical integration. Eur Respir J 2009; 33(1):201–212.
66. Imamura Y, Azuma K, Kurata S, Hattori S, Sasada T, Kinoshita T, Okamoto M, Kawayama T, Kaida H, Ishibashi M and Aizawa H. Prognostic value of SUVmax measurements obtained by FDG-PET in patients with non-small cell lung cancer receiving chemotherapy. Lung Cancer 2011; 71(1):49–54.
67. Casali C, Cucca M, Rossi G, Barbieri F, Iacuzio L, Bagni B and Uliano M. The variation of prognostic significance of Maximum Standardized Uptake Value of [18F]-fluoro-2-deoxy-glucose positron emission tomography in different histological subtypes and pathological stages of surgically resected Non-Small Cell Lung Carcinoma. Lung Cancer 2010; 69(2):187–193.
68. Goudarzi B, Jacene HA and Wahl RL. Diagnosis and differentiation of bronchioloalveolar carcinoma from adenocarcinoma with bronchioloalveolar components with metabolic and anatomic characteristics using PET/CT. J Nucl Med 2008; 49(10):1585–1592.
69. Taylor C, Munro AJ, Glynne-Jones R, Griffith C, Trevatt P, Richards M and Ramirez AJ. Multidisciplinary team working in cancer: what is the evidence? BMJ 2010; 340:c951.
70. Tho L and Wong D. Delivering cancer services: a multi-disciplinary approach. Biomed Imaging Interv J 2006; 2(2):e31.
71. Shim SS, Lee KS, Kim BT, Chung MJ, Lee EJ, Han J, Choi JY, Kwon OJ, Shim YM and Kim S. Non-small cell lung cancer: prospective comparison of integrated FDG PET/CT and CT alone for preoperative staging. Radiology 2005; 236(3):1011–1019.
72. Pauls S, Buck AK, Hohl K, Halter G, Hetzel M, Blumstein NM, Mottaghy FM, Glatting G, Krüger S, Sunder-Plassmann L, Möller P, Hombach V, Brambs HJ and Reske SN. Improved non-invasive T-Staging in non-small cell lung cancer by integrated 18F-FDG PET/CT. Nuklearmedizin 2007; 46(1):9–14; quiz N11-12.
73. Lardinois D, Weder W, Hany TF, Kamel EM, Korom S, Seifert B, von Schulthess GK and Steinert HC. Staging of non-small-cell lung cancer with integrated positron-emission tomography and computed tomography. N Engl J Med 2003; 348(25):2500–2507.
74. Erasmus JJ, McAdams HP, Rossi SE, Goodman PC, Coleman RE and Patz EF. FDG PET of pleural effusions in patients with non-small cell lung cancer. AJR Am J Roentgenol 2000; 175(1):245–249.
75. Schaffler GJ, Wolf G, Schoellnast H, Groell R, Maier A, Smolle-Jüttner FM, Woltsche M, Fasching G, Nicoletti R and Aigner RM. Non-small cell lung cancer: evaluation of pleural abnormalities on CT scans with 18F FDG PET. Radiology 2004; 231(3):858–865.
76. Berghmans T, Dusart M, Paesmans M, Hossein-Foucher C, Buvat I, Castaigne C, Scherpereel A, Mascaux C, Moreau M, Roelandts M, Alard S, Meert AP, Patz EF Jr, Lafitte JJ, Sculier JP and European Lung Cancer Working Party for the IASLC Lung Cancer Staging Project. Primary tumor standardized uptake value (SUVmax) measured on fluorodeoxyglucose positron emission tomography (FDG-PET) is of prognostic value for survival in non-small cell lung cancer (NSCLC): a systematic review and meta-analysis (MA) by the European Lung Cancer Working Party for the IASLC Lung Cancer Staging Project. J Thorac Oncol 2008; 3(1):6–12.
77. Downey RJ, Akhurst T, Gonen M, Park B and Rusch V. Fluorine-18 fluorodeoxyglucose positron emission tomographic maximal standardized uptake value predicts survival independent of clinical but not pathologic TNM staging of resected non-small cell lung cancer. J Thorac Cardiovasc Surg 2007; 133(6):1419–1427.
78. Nomori H, Watanabe K, Ohtsuka T, Naruke T, Suemasu K, Kobayashi T and Uno K. Fluorine 18-tagged fluorodeoxyglucose positron emission tomographic scanning to predict lymph node metastasis, invasiveness, or both, in clinical T1 N0 M0 lung adenocarcinoma. J Thorac Cardiovasc Surg 2004; 128(3):396–401.
79. Lv YL, Yuan DM, Wang K, Miao XH, Qian Q, Wei SZ, Zhu XX and Song Y. Diagnostic performance of integrated positron emission tomography/computed tomography for mediastinal lymph node staging in non-small cell lung cancer: a bivariate systematic review and meta-analysis. J Thorac Oncol 2011; 6(8):1350–1358.
80. Birim O, Kappetein AP, Stijnen T and Bogers AJ. Meta-analysis of positron emission tomographic and computed tomographic

imaging in detecting mediastinal lymph node metastases in nonsmall cell lung cancer. Ann Thorac Surg 2005; 79(1):375–382.
81. Crinò L, Weder W, van Meerbeeck J, Felip E and ESMO Guidelines Working Group. Early stage and locally advanced (non-metastatic) non-small-cell lung cancer: ESMO Clinical Practice Guidelines for diagnosis, treatment and follow-up. Ann Oncol 2010; 21(Suppl 5):v103–v115.
82. Darling GE, Maziak DE, Inculet RI, Gulenchyn KY, Driedger AA, Ung YC, Gu CS, Kuruvilla MS, Cline KJ, Julian JA, Evans WK and Levine MN. Positron Emission Tomography-Computed Tomography Compared with Invasive Mediastinal Staging in Non-small Cell Lung Cancer: Results of Mediastinal Staging in the Early Lung Positron Emission Tomography Trial. J Thorac Oncol 2011; 6(8):1367–1372.
83. Detterbeck FC, Jantz MA, Wallace M, Vansteenkiste J, Silvestri GA and American College of Chest Physicians. Invasive mediastinal staging of lung cancer: ACCP evidence-based clinical practice guidelines (2nd edition). Chest 2007; 132(Suppl 3):202S-220S.
84. Gómez-Caro A, Garcia S, Reguart N, Arguis P, Sanchez M, Gimferrer JM, Marrades R and Lomeña F. Incidence of occult mediastinal node involvement in cN0 non-small-cell lung cancer patients after negative uptake of positron emission tomography/computer tomography scan. Eur J Cardiothorac Surg 2010; 37(5):1168–1174.
85. Cerfolio RJ, Bryant AS, Ojha B and Eloubeidi M. Improving the inaccuracies of clinical staging of patients with NSCLC: a prospective trial. Ann Thorac Surg 2005; 80(4):1207–1213; discussion 1213–1204.
86. Eschmann SM, Friedel G, Paulsen F, Budach W, Harer-Mouline C, Dohmen BM and Bares R. FDG PET for staging of advanced non-small cell lung cancer prior to neoadjuvant radio-chemotherapy. Eur J Nucl Med Mol Imaging 2002; 29(6):804–808.
87. MacManus MP, Hicks RJ, Matthews JP, Hogg A, McKenzie AF, Wirth A, Ware RE and Ball DL. High rate of detection of unsuspected distant metastases by pet in apparent stage III non-small-cell lung cancer: implications for radical radiation therapy. Int J Radiat Oncol Biol Phys 2001; 50(2):287–293.
88. Shekhar R, Walimbe V, Raja S, Zagrodsky V, Kanvinde M, Wu G and Bybel B. Automated 3-dimensional elastic registration of whole-body PET and CT from separate or combined scanners. J Nucl Med 2005; 46(9):1488–1496.
89. Langen KM and Jones DT. Organ motion and its management. Int J Radiat Oncol Biol Phys 2001; 50(1):265–278.
90. Matsopoulos GK, Mouravliansky NA, Asvestas PA, Delibasis KK and Kouloulias V. Thoracic non-rigid registration combining self-organizing maps and radial basis functions. Med Image Anal 2005; 9(3):237–254.
91. Orban de Xivry J, Janssens G, Bosmans G, De Craene M, Dekker A, Buijsen J, van Baardwijk A, De Ruysscher D, Macq B and Lambin P. Tumour delineation and cumulative dose computation in radiotherapy based on deformable registration of respiratory correlated CT images of lung cancer patients. Radiother Oncol 2007; 85(2):232–238.
92. Grgic A, Nestle U, Schaefer-Schuler A, Kremp S, Ballek E, Fleckenstein J, Rübe C, Kirsch CM and Hellwig D. Nonrigid versus rigid registration of thoracic 18F-FDG PET and CT in patients with lung cancer: an intraindividual comparison of different breathing maneuvers. J Nucl Med 2009; 50(12):1921–1926.
93. Al-Mayah A, Moseley J, Velec M and Brock K. Toward efficient biomechanical-based deformable image registration of lungs for image-guided radiotherapy. Phys Med Biol 2011; 56(15):4701–4713.
94. Wu J, Lei P, Shekhar R, Li H, Suntharalingam M and D'Souza WD. Do tumors in the lung deform during normal respiration? An image registration investigation. Int J Radiat Oncol Biol Phys 2009; 75(1):268–275.
95. De Ruysscher D and Kirsch CM. PET scans in radiotherapy planning of lung cancer. Radiother Oncol 2010; 96(3):335–338.
96. Senan S, De Ruysscher D, Giraud P, Mirimanoff R, Budach V and Radiotherapy Group of European Organization for Research and Treatment of Cancer. Literature-based recommendations for treatment planning and execution in high-dose radiotherapy for lung cancer. Radiother Oncol 2004; 71(2):139–146.
97. Mah K, Caldwell CB, Ung YC, Danjoux CE, Balogh JM, Ganguli SN, Ehrlich LE and Tirona R. The impact of (18)FDG-PET on target and critical organs in CT-based treatment planning of patients with poorly defined non-small-cell lung carcinoma: a prospective study. Int J Radiat Oncol Biol Phys 2002; 52(2):339–350.
98. Munley MT, Marks LB, Scarfone C, Sibley GS, Patz EF Jr, Turkington TG, Jaszczak RJ, Gilland DR, Anscher MS and Coleman RE. Multimodality nuclear medicine imaging in three-dimensional radiation treatment planning for lung cancer: challenges and prospects. Lung Cancer 1999; 23(2):105–114.
99. Nestle U, Walter K, Schmidt S, Licht N, Nieder C, Motaref B, Hellwig D, Niewald M, Ukena D, Kirsch CM, Sybrecht GW and Schnabel K. 18F-deoxyglucose positron emission tomography (FDG-PET) for the planning of radiotherapy in lung cancer: high impact in patients with atelectasis. Int J Radiat Oncol Biol Phys 1999; 44(3):593–597.
100. Vanuytsel LJ, Vansteenkiste JF, Stroobants SG, De Leyn PR, De Wever W, Verbeken EK, Gatti GG, Huyskens DP and Kutcher GJ. The impact of (18)F-fluoro-2-deoxy-D-glucose positron emission tomography (FDG-PET) lymph node staging on the radiation treatment volumes in patients with non-small cell lung cancer. Radiother Oncol 2000; 55(3):317–324.
101. Van de Steene J, Linthout N, de Mey J, Vinh-Hung V, Claassens C, Noppen M, Bel A and Storme G. Definition of gross tumor volume in lung cancer: inter-observer variability. Radiother Oncol 2002; 62(1):37–49.
102. Senan S, van Sörnsen de Koste J, Samson M, Tankink H, Jansen P, Nowak PJ, Krol AD, Schmitz P and Lagerwaard FJ. Evaluation of a target contouring protocol for 3D conformal radiotherapy in non-small cell lung cancer. Radiother Oncol 1999; 53(3):247–255.
103. Hanna GG, McAleese J, Carson KJ, Stewart DP, Cosgrove VP, Eakin RL, Zatari A, Lynch T, Jarritt PH, Young VA, O'Sullivan JM and Hounsell AR. (18)F-FDG PET-CT simulation for non-small-cell lung cancer: effect in patients already staged by PET-CT. Int J Radiat Oncol Biol Phys 2010; 77(1):24–30.
104. Fox JL, Rengan R, O'Meara W, Yorke E, Erdi Y, Nehmeh S, Leibel SA and Rosenzweig KE. Does registration of PET and planning CT images decrease interobserver and intraobserver variation in delineating tumor volumes for non-small-cell lung cancer? Int J Radiat Oncol Biol Phys 2005; 62(1):70–75.
105. van Herk M. Errors and margins in radiotherapy. Semin Radiat Oncol 2004; 14(1):52–64.
106. Mutic S, Dempsey JF, Bosch WR, Low DA, Drzymala RE, Chao KS, Goddu SM, Cutler PD and Purdy JA. Multimodality image registration quality assurance for conformal three-dimensional treatment planning. Int J Radiat Oncol Biol Phys 2001; 51(1):255–260.
107. Ashamalla H, Rafla S, Parikh K, Mokhtar B, Goswami G, Kambam S, Abdel-Dayem H, Guirguis A, Ross P and Evola A. The contribution of integrated PET/CT to the evolving definition of treatment volumes in radiation treatment planning in lung cancer. Int J Radiat Oncol Biol Phys 2005; 63(4):1016–1023.
108. Paulino AC and Johnstone PA. FDG-PET in radiotherapy treatment planning: Pandora's box? Int J Radiat Oncol Biol Phys 2004; 59(1):4–5.
109. Bradley J, Thorstad WL, Mutic S, Miller TR, Dehdashti F, Siegel BA, Bosch W and Bertrand RJ. Impact of FDG-PET on radiation therapy volume delineation in non-small-cell lung cancer. Int J Radiat Oncol Biol Phys 2004; 59(1):78–86.
110. Erdi YE, Rosenzweig K, Erdi AK, Macapinlac HA, Hu YC, Braban LE, Humm JL, Squire OD, Chui CS, Larson SM and Yorke ED. Radiotherapy treatment planning for patients with non-small cell lung cancer using positron emission tomography (PET). Radiother Oncol 2002; 62(1):51–60.
111. Biehl KJ, Kong FM, Dehdashti F, Jin JY, Mutic S, El Naqa I, Siegel BA and Bradley JD. 18F-FDG PET definition of gross tumor volume for radiotherapy of non-small cell lung cancer: is a single standardized uptake value threshold approach appropriate? J Nucl Med 2006; 47(111):1808–1812.
112. Black QC, Grills IS, Kestin LL, Wong CY, Wong JW, Martinez AA and Yan D. Defining a radiotherapy target with positron emission tomography. Int J Radiat Oncol Biol Phys 2004; 60(4):1272–1282.
113. Daisne JF, Sibomana M, Bol A, Doumont T, Lonneux M and Grégoire V. Tri-dimensional automatic segmentation of PET volumes based on measured source-to-background ratios: influence of reconstruction algorithms. Radiother Oncol 2003; 69(3):247–250.
114. Nestle U, Kremp S, Schaefer-Schuler A, Sebastian-Welsch C, Hellwig D, Rübe C and Kirsch CM. Comparison of different

methods for delineation of 18F-FDG PET-positive tissue for target volume definition in radiotherapy of patients with non-Small cell lung cancer. J Nucl Med 2005; 46(8):1342–1348.

115. Chinneck CD, McJury M and Hounsell AR. The potential for undertaking slow CT using a modern CT scanner. Br J Radiol 2010; 83(992):687–693.
116. Nehmeh SA, Erdi YE, Ling CC, Rosenzweig KE, Schoder H, Larson SM, Macapinlac HA, Squire OD and Humm JL. Effect of respiratory gating on quantifying PET images of lung cancer. J Nucl Med 2002; 43(7):876–881.
117. Erdi YE, Nehmeh SA, Pan T, Pevsner A, Rosenzweig KE, Mageras G, Yorke ED, Schoder H, Hsiao W, Squire OD, Vernon P, Ashman JB, Mostafavi H, Larson SM and Humm JL. The CT motion quantitation of lung lesions and its impact on PET-measured SUVs. J Nucl Med 2004; 45(8):1287–1292.
118. Nehmeh SA and Erdi YE. Respiratory motion in positron emission tomography/computed tomography: a review. Semin Nucl Med 2008; 38(3):167–176.
119. Park SJ, Ionascu D, Killoran J, Mamede M, Gerbaudo VH, Chin L and Berbeco R. Evaluation of the combined effects of target size, respiratory motion and background activity on 3D and 4D PET/CT images. Phys Med Biol 2008; 53(13):3661–3679.
120. Vines DC, Keller H, Hoisak JD and Breen SL. Quantitative PET comparing gated with nongated acquisitions using a NEMA phantom with respiratory-simulated motion. J Nucl Med Technol 2007; 35(4):246–251.
121. Board of the Faculty of Clinical Oncology. Imaging for Oncology: Collaboration between Clinical Radiologists and Clinical Oncologists in Diagnosis, Staging and Radiotherapy Planning. London: The Royal College of Radiologists, 2004.
122. Ginat DT, Fong MW, Tuttle DJ, Hobbs SK and Vyas RC. Cardiac imaging: Part 1, MR pulse sequences, imaging planes, and basic anatomy. AJR Am J Roentgenol 2011; 197(4):808–815.
123. Plathow C, Ley S, Fink C, Puderbach M, Hosch W, Schmähl A, Debus J and Kauczor HU. Analysis of intrathoracic tumor mobility during whole breathing cycle by dynamic MRI. Int J Radiat Oncol Biol Phys 2004; 59(4):952–959.
124. Blackall JM, Ahmad S, Miquel ME, McClelland JR, Landau DB and Hawkes DJ. MRI-based measurements of respiratory motion variability and assessment of imaging strategies for radiotherapy planning. Phys Med Biol 2006; 51(17):4147–4169.
125. Remmert G, Biederer J, Lohberger F, Fabel M and Hartmann GH. Four-dimensional magnetic resonance imaging for the determination of tumour movement and its evaluation using a dynamic porcine lung phantom. Phys Med Biol 2007; 52(18):N401–N415.
126. Biederer J, Dinkel J, Remmert G, Jetter S, Nill S, Moser T, Bendl R, Thierfelder C, Fabel M, Oelfke U, Bock M, Plathow C, Bolte H, Welzel T, Hoffmann B, Hartmann G, Schlegel W, Debus J, Heller M and Kauczor HU. 4D-Imaging of the lung: reproducibility of lesion size and displacement on helical CT, MRI, and cone beam CT in a ventilated ex vivo system. Int J Radiat Oncol Biol Phys 2009; 73(3):919–926.
127. Wild JM, Woodhouse N, Paley MN, Fichele S, Said Z, Kasuboski L and van Beek EJ. Comparison between 2D and 3D gradient-echo sequences for MRI of human lung ventilation with hyperpolarized 3He. Magn Reson Med 2004; 52(3):673–678.
128. Kauczor HU, Chen XJ, van Beek EJ and Schreiber WG. Pulmonary ventilation imaged by magnetic resonance: at the doorstep of clinical application. Eur Respir J 2001; 17(5):1008–1023.
129. Ireland RH, Bragg CM, McJury M, Woodhouse N, Fichele S, van Beek EJ, Wild JM and Hatton MQ. Feasibility of image registration and intensity-modulated radiotherapy planning with hyperpolarized helium-3 magnetic resonance imaging for non-small-cell lung cancer. Int J Radiat Oncol Biol Phys 2007; 68(1):273–281.
130. Allen AM, Albert M, Caglar HB, Zygmanski P, Soto R, Killoran J and Sun Y. Can Hyperpolarized Helium MRI add to radiation planning and follow-up in lung cancer? J Appl Clin Med Phys 2011; 12(2):3357.